

## **A DUAL-BAND IMPEDANCE TRANSFORMING TECHNIQUE WITH LUMPED ELEMENTS FOR FREQUENCY-DEPENDENT COMPLEX LOADS**

**Byeong-Taek Moon\*** and Noh-Hoon Myung

Department of Electrical Engineering, Korea Advanced Institute of Science and Technology (KAIST), 291 Daehak-ro, Yuseong-gu, Daejeon 305-701, Rep. of Korea

**Abstract**—In this paper, a new technique to realize lumped dual-band impedance transformers for arbitrary frequency-dependent complex loads is proposed. For the complex impedance transforming, closed-form design equations are presented for a series-shunt and a shunt-series type and a concept of combination is also presented. They use the proposed equation of input impedance. This equation can easily and exactly obtain the input impedance of any two-port network using the *ABCD* matrix. Then in order to realize dual-band operation, four topologies comprising two types and a design method are presented. This technique is numerically demonstrated by various examples with excellent results and it has advantages of simplicity, intuitiveness and versatility because it is a general solution for complex impedance transforming. The proposed dual-band impedance transforming technique can be utilized for practical matching problems such as microwave amplifiers and other devices.

### **1. INTRODUCTION**

Impedance transformers are basic and important devices in microwave systems. Among other things, the quarter-wavelength transmission is the most widely used impedance transformer designed for single band operation. However, recently, dual-band circuits and systems have become required and thus the demand for dual-band impedance transformers has been increasing. With the necessity of dual-band operation, many researchers have increasingly focused on dual-band impedance transformers. In order to realize the dual-band

---

*Received 18 November 2012, Accepted 7 January 2013, Scheduled 16 January 2013*

\* Corresponding author: Byeong-Taek Moon (btmoon@kaist.ac.kr).

transformer, Chow and Wan [1] firstly developed a dual-band two-section transformer that operates at a frequency and its first harmonic for a real impedance load. Mozon [2] proposed a dual-band two-section transformer at two arbitrary frequencies. Wu et al. [3] modified the dual-band transformer [2] using a pi-structure for compact size. Sophocles and Orfanidis [4] and Castaldi et al. [5] proposed dual-band transformers with Chebyshev response. These dual-band transformers are realized for a real impedance load at two designated frequencies. Hence, they are applicable in passive circuits such as dual-band filters, dual-band power dividers and so forth [6–9]. In terms of active circuits, complex impedance transformers are required such as a dual-band amplifier [10–12]. Wu et al. [13] extended a two-section transformer to deal with equal complex loads at two frequencies using unequal transmission lines. Liu et al. [14] proposed a dual-band three-section transformer for frequency-dependent complex loads and Chuang [15] proposed a dual-band transformer that consists of a two-section transmission line and a two-section shunt stub. A T-section dual-band transformer was also introduced by Nikravan and Atlasbaf [16]. For operating at two relatively close operating frequencies, Li et al. [17] presented a dual-band coupled-line transformer. The above dual-band impedance transformers use distributed elements such as the transmission line and the shunt stub, thus they are always bulky, especially in the microwave region. Recently, a lumped type of dual-band impedance transformer was developed by Liu et al. [18] for decreasing the circuit size. [18] proposed only three structures with lumped elements for frequency-dependent complex loads and adopted extended the impedance matching concept of L-type networks that uses graphical approach in Smith chart.

This paper proposes a new dual-band impedance transforming technique, which uses the proposed equation of input impedance for exact analytical solutions. This equation can easily and exactly obtain the input impedance of any two-port network using  $ABCD$  matrix for the complex impedance transforming. The proposed dual-band impedance transforming technique can realize frequency-dependent complex impedance matching at any two arbitrary frequencies. For the complex impedance transformer using the lumped elements, a series-shunt and a shunt-series type are presented with closed-form design equations and a concept of combination is also presented. Then, these types are comprised of four topologies to realize dual-band operation. According to the proposed technique, general solutions of the lumped dual-band transformer can be obtained for various structures with limited number of lumped elements. The feasibility and the versatility of the proposed dual-band impedance transforming

technique are numerically demonstrated by various examples.

## 2. INPUT IMPEDANCE FOR COMPLEX IMPEDANCE TRANSFORMING

Complex impedance transforming is matching from complex load to required source which is generally  $50\Omega$ . The equation of the input impedance of a transmission line is widely used when distributed elements are used to realize the impedance transformer. However, a general equation of the input impedance does not exist when lumped elements are used for complex impedance transforming. Hence, an equation is proposed that introduces calculating the input impedance of any two-port network for complex impedance transforming.

### 2.1. Converted from $ABCD$ Matrix to $S$ -matrix in General Case and Reference Impedance

General input impedance of the two-port network is given by the following well known equation:

$$Z_{in} = Z_0 \frac{1 + \Gamma}{1 - \Gamma} \quad (1)$$

where  $\Gamma = S_{11} + S_{12}S_{21}\Gamma_L/(1 - S_{22}\Gamma_L)$ ,  $Z_0$  is the characteristic impedance of the two-port network, and  $\Gamma_L$  is the reflection coefficient at the load. In order to obtain the perfect matching,  $\Gamma_L$  should be equal to zero. Hence,  $\Gamma = S_{11}$  and then  $Z_{in}$  can be calculated by  $S_{11}$  where ports 1 and 2 are input and load, respectively.  $S_{11}$  can then be calculated as [19]

$$\begin{bmatrix} S_{11} & S_{12} \\ S_{21} & S_{22} \end{bmatrix} = \frac{1}{A + B/Z_r + CZ_r + D} \begin{bmatrix} A + B/Z_r - CZ_r - D & 2(AD - BC) \\ 2 & -A + B/Z_r - CZ_r + D \end{bmatrix} \quad (2)$$

where  $Z_r$  is reference impedance to convert from  $ABCD$  matrix to  $S$ -matrix. Equation (2) is valid when  $Z_r$  is equal to  $Z_0$ , which is the real characteristic impedance, and they are equal to the terminated impedance of ports 1 and 2. For this reason, Equation (2) cannot be used to calculate the input impedance for the complex impedance transforming. Hence, Equation (2) should be modified by a new definition of  $Z_r$  to realize the complex impedance transformer with the lumped elements. The new definition of  $Z_r$  will be explained in the following section.

## 2.2. Converted from $ABCD$ Matrix to $S$ -matrix for Complex Impedance Transforming

Current and voltage of the two-port network at each ports are can be obtained as [20]

$$I_i = \frac{2\sqrt{|\operatorname{Re}Z_{ri}|}(a_i - b_i)}{Z_{ri} + Z_{ri}^*}, \quad i = 1, 2 \quad (3)$$

$$V_i = \frac{2\sqrt{|\operatorname{Re}Z_{ri}|}(a_i Z_{ri}^* + b_i Z_{ri})}{Z_{ri} + Z_{ri}^*}, \quad i = 1, 2 \quad (4)$$

where  $i$  is the port number in the two-port network.  $a_i$  and  $b_i$  are incident and reflected wave, respectively. The reference impedances can have any values [20], thus we assume that  $Z_{r1}$  is real and  $Z_{r2}$  is complex for complex impedance transforming. In order to obtain  $S_{11}$ , parameters of  $ABCD$  matrix can be calculated by (3) and (4) as

$$\begin{aligned} A &= \left. \frac{V_1}{V_2} \right|_{I_2=0} = \sqrt{\frac{R_{r1}}{R_{r2}}} \frac{a_1 + b_1}{2a_2}, & B &= \left. \frac{V_1}{I_2} \right|_{V_2=0} = \sqrt{R_{r1}R_{r2}} \frac{Z_{r2}}{Z_{r2}^*} \frac{a_1 + b_1}{2a_2} \\ C &= \left. \frac{I_1}{V_2} \right|_{I_2=0} = \frac{1}{\sqrt{R_{r1}R_{r2}}} \frac{a_1 - b_1}{2a_2}, & D &= \left. \frac{I_1}{I_2} \right|_{V_2=0} = \sqrt{\frac{R_{r2}}{R_{r1}}} \frac{Z_{r2}}{Z_{r2}^*} \frac{a_1 - b_1}{2a_2} \end{aligned} \quad (5)$$

According to Equation (5),  $S_{11}$  can be calculated as

$$S_{11} = \frac{b_1}{a_1} = \frac{\sqrt{\frac{R_{r2}}{R_{r1}}} + B/\sqrt{R_{r1}R_{r2}}/Z'_{r2} - C\sqrt{R_{r1}R_{r2}} - D\sqrt{\frac{R_{r1}}{R_{r2}}}/Z'_{r2}}{\sqrt{\frac{R_{r2}}{R_{r1}}} + B/\sqrt{R_{r1}R_{r2}}/Z'_{r2} + C\sqrt{R_{r1}R_{r2}} + D\sqrt{\frac{R_{r1}}{R_{r2}}}/Z'_{r2}} \quad (6)$$

where  $Z'_{r2}$  is  $Z_{r2}/Z_{r2}^*$ . Hence, the input impedance for the complex impedance transforming can be obtained as

$$Z_{in} = Z_0 \frac{1 + S_{11}}{1 - S_{11}} = Z_0 \frac{AR_{r2}Z'_{r2} + B}{DR_{r1} + CR_{r1}R_{r2}Z'_{r2}} \quad (7)$$

Equation (7) can be used for calculating the input impedance of any two-port network such as transmission line. Hence, conventional input impedance of the transmission line should be equal to the input impedance of Equation (7) using the  $ABCD$  matrix of the transmission line. The expression can be written as

$$Z_{in} = Z_0 \frac{Z_L + jZ_0 \tan \theta}{Z_0 + jZ_L \tan \theta} = Z_0 \frac{R_{r2}Z'_{r2} + jZ_0 \tan \theta}{R_{r1} + jY_0 R_{r1} R_{r2} Z'_{r2} \tan \theta} \quad (8)$$

According to Equation (8), the reference impedances can be defined as

$$Z_{r1} = Z_0, \quad R_{r2}Z'_{r2} = Z_L \quad (9)$$

where  $Z_0$  is the characteristic impedance of the two-port network and  $Z_L$  the complex load impedance. Hence,  $Z_{r1}$  is real and  $Z_{r2}$  is complex, and thus the assumption is correct. Finally, the input impedance of the two-port network using  $ABCD$  matrix can be obtained by substituting (9) into (7) and following the equation is given as

$$Z_{in} = \frac{AZ_L + B}{D + CZ_L} \tag{10}$$

Equation (10) easily calculates the input impedance using the  $ABCD$  matrix and can be used in any two-port network for complex impedance transforming. Hence, this equation is used for the dual-band complex impedance transformer.

### 3. DUAL-BAND IMPEDANCE TRANSFORMING TECHNIQUE

A lumped dual-band impedance transformer can have various structures depending on the configuration of lumped elements. Hence, two types of the transformer are presented to generalize the complex impedance transformer with the lumped elements. They are a series-shunt and shunt-series type, and combinations of these two types are also presented. Then, these types only provide the parameters of the whole structure for complex impedance transforming. Thus, in order to realize dual-band operation, topologies comprising the two types should be defined. Hence, we present four topologies that are composite right/left-handed transmission line (CRLH TL) [21], dual-CRLH TL (D-CRLH TL) [22], series resonance and parallel resonance topology.

#### 3.1. Series-shunt Type and Closed-form Design Equation

Figure 1 shows a series-shunt type of dual-band impedance transformer. Series impedance and shunt admittance are cascaded and input is in the direction of the series impedance. Then, a complex load impedance is  $Z_L = R_L + jX_L$ .

The  $ABCD$  matrix of the series-shunt type can be obtained as

$$\begin{bmatrix} 1 - X_p X_q & jX_p \\ jX_q & 1 \end{bmatrix} \tag{11}$$

where  $jX_p = Z$  and  $jX_q = Y$ . The input impedance using  $ABCD$  matrix can be easily calculated by (10). Hence, the input impedance of the series-shunt type can be obtained as

$$Z_{in} = \frac{R_L + j \{X_L - X_L^2 X_q - R_L^2 X_q + (1 - 2X_L X_q + R_L^2 X_q^2 + X_L^2 X_q^2) X_p\}}{(1 - X_L X_q)^2 + (R_L X_q)^2} \tag{12}$$

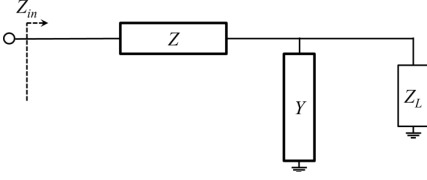


**Figure 1.** Series-shunt type of dual-band impedance transformer.

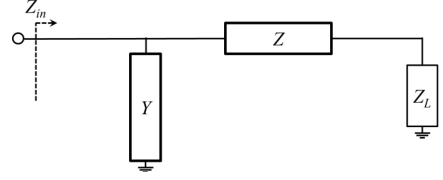


**Figure 2.** Shunt-series type of dual-band impedance transformer.

The input impedance is separated into real and imaginary parts. In the real part,  $X_q$  is only an unknown value and thus  $X_q$  can be calculated as

$$X_q = \frac{R_{in}X_L \pm \sqrt{R_{in}R_L(R_L^2 + X_L^2 - R_{in}R_L)}}{R_{in}(R_L^2 + X_L^2)} \quad (13)$$

where  $X_q$  is real and thus  $R_L - R_{in} + X_L^2/R_L > 0$ . In the imaginary part,  $X_p$  is obtained, and a denominator is  $R_L/R_{in}$  that is a known value according to the real part. Hence,  $X_p$  can be calculated as

$$X_p = \frac{(R_L^2 + X_L^2)X_q - X_L + \frac{X_{in}}{R_{in}}R_L}{(R_L^2 + X_L^2)X_q^2 - 2X_LX_q + 1} \quad (14)$$

Hence, the unknown values,  $X_p$  and  $X_q$ , are obtained in the series-shunt type and thus according to the kind of topology, only  $X_p$  and  $X_q$  have to be used.

### 3.2. Shunt-series Type and Closed-form Design Equation

Figure 2 shows a shunt-series type of dual-band impedance transformer. Shunt admittance and series impedance cascaded and input is in the direction of the shunt admittance. Then, a complex load impedance is  $Z_L = R_L + jX_L$ .

The  $ABCD$  matrix of the shunt-series type can be similarly obtained as

$$\begin{bmatrix} 1 & jX_p \\ jX_q & 1 - X_pX_q \end{bmatrix} \quad (15)$$

The input impedance of the shunt-series type is calculated by (10) as

$$Z_{in} = \frac{R_L + j\{(X_L + X_p + (-R_L^2 - (X_L + X_p)^2)X_q)\}}{(1 - X_pX_q - X_LX_q)^2 + (R_LX_q)^2} \quad (16)$$

Real and imaginary parts consist of  $X_p$  and  $X_q$ , respectively and then a denominator is  $R_L/R_{in}$  that is a known value according to the real part. In the imaginary part, an equation of  $X_q$  can be made by rearrangement as

$$X_q = \frac{X_L + X_p - \frac{X_{in}}{R_{in}} R_L}{(X_L + X_p)^2 + R_L^2} \quad (17)$$

Equation (17) is substituted into the real part. Then, the real part has only one unknown value of  $X_p$ , and thus  $X_p$  can be calculated as

$$X_p = -X_L \pm \sqrt{R_L \left( R_{in} - R_L + \frac{X_{in}^2}{R_{in}} \right)} \quad (18)$$

where  $X_p$  is real and thus  $R_{in} - R_L + X_{in}^2/R_{in} > 0$ . Hence, the unknown values, which are  $X_p$  and  $X_q$ , are obtained in the shunt-series type.

### 3.3. Combinations of Series-shunt and Shunt-series Type

Two types of dual-band impedance transformer, which are the series-shunt and the shunt-series type, can obtain most solutions for various complex loads. However, they cannot be obtained for a precious few complex loads because the radicand in  $X_p$  and  $X_q$  should be always a positive value in (13), (18). Here, in order to solve this problem, a concept of combination is proposed. The combination is a two-stage impedance transformer using the series-shunt and the shunt-series type. Figure 3 shows the T-type combination that the series-shunt and the shunt-series type are cascaded. Figure 4 shows the  $\pi$ -type combination that the shunt-series and the series-shunt type are cascaded. This concept of combinations is simple. The complex load is matched to  $Z_{in2}$  at midpoint, and then  $Z_{in2}$  is matched to  $Z_{in1}$ , and then  $Z_{in1}$  is required input impedance which is generally  $50 \Omega$ . While the number of the lumped elements is increased, these combinations provide more flexible solutions. Then, the number of lumped elements of impedances or admittances at midpoint can be reduced when  $Y_{ses}$  and  $Y_{shs}$  are only parallel resonance and  $Z_{ses}$  and  $Z_{shs}$  are only series resonance such as CRLH TL topology. The concept of these combinations provides applicability and extendibility of the proposed design method using closed-form equations of the series-shunt and the shunt-series type.

### 3.4. Topologies and Analysis for Dual-band Operation

For the complex impedance transforming, two types of the impedance transformer were presented. Then, in order to realize the dual-band

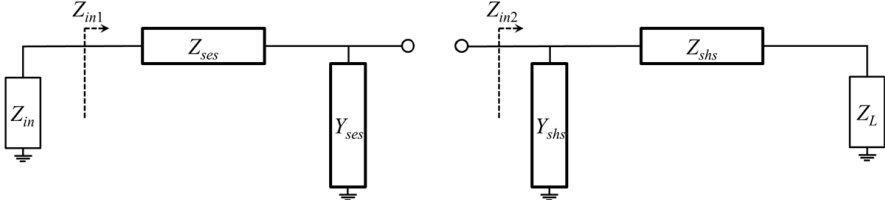


**Figure 3.** T-type combination.

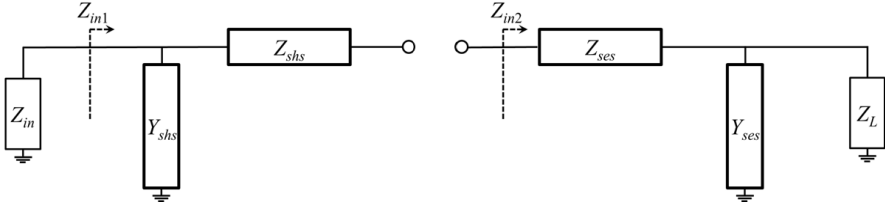


**Figure 4.**  $\pi$ -type combination.

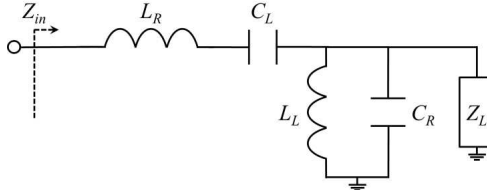


**Figure 5.** CRLH TL topology for dual-band impedance transformer.

operation, these two types are comprised of four topologies, which are CRLH TL, D-CRLH TL, series resonance and parallel resonance topology. Figure 5 shows the CRLH TL topology of the series-shunt type.

The CRLH TL has a band-pass characteristic and consists of series resonance at series connection and parallel resonance at shunt connection. Hence, the impedance of  $Z$  and the admittance of  $Y$  are obtained as

$$Z = jX_p = j \left( \omega_s L_R - \frac{1}{\omega_s C_L} \right), \quad Y = jX_q = j \left( \omega_s C_R - \frac{1}{\omega_s L_L} \right) \quad (19)$$

where  $\omega_s$  is the solution angular frequency. These  $X_p$ ,  $X_q$  can be calculated by (13), (14) because of series-shunt type and they have two values at two arbitrary frequencies for the dual-band operation, respectively because of frequency-dependent complex impedance loads.

Hence,  $X_{p1}$  and  $X_{q2}$  can be obtained as

$$X_{p1} = \omega_s L_R - \frac{1}{\omega_s C_L}, \quad \text{at } f_{s1} \quad (20a)$$

$$X_{p2} = K\omega_s L_R - \frac{1}{K\omega_s C_L}, \quad \text{at } f_{s2} \quad (20b)$$

where  $K$  is frequency ratio,  $K = f_{s2}/f_{s1} = \omega_{s2}/\omega_s$ ,  $K \geq 1$ .  $f_{s1}$  and  $f_{s2}$  are a first and a second frequency, respectively. According to Equation (20),  $C_L$  and  $L_R$  can be calculated and  $L_L$  and  $C_R$  can be also calculated by  $X_q$  using the same design process. Hence, the component values ( $C_R$ ,  $C_L$ ,  $L_R$ ,  $L_L$ ) of the CRLH TL topology can be obtained as

$$C_R = \frac{1}{\omega_s} \left( X_{q1} + \frac{1}{\omega_s L_L} \right) \quad (21a)$$

$$C_L = \frac{K^2 - 1}{\omega_s K (X_{p2} - K X_{p1})} \quad (21b)$$

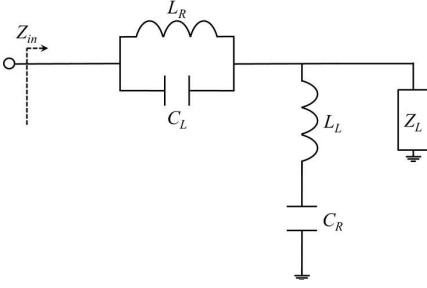
$$L_R = \frac{1}{\omega_s} \left( X_{p1} + \frac{1}{\omega_s C_L} \right) \quad (21c)$$

$$L_L = \frac{K^2 - 1}{\omega_s K (X_{q2} - K X_{q1})} \quad (21d)$$

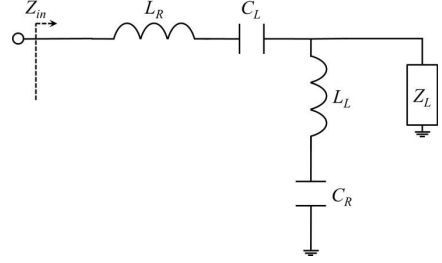
The CRLH TL topology of the shunt-series also uses Equation (21) to calculate component values of the CRLH TL. Here,  $X_{p1}$ ,  $X_{p2}$ ,  $X_{q1}$  and  $X_{q2}$  have two solutions at a frequency, respectively because of (13), (18) and thus the combination of  $X_{p1}$  and  $X_{p2}$ , and the combination of  $X_{q1}$  and  $X_{q2}$  have four solutions, respectively. Hence, according to Equation (21), these component values of the CRLH TL topology can have four solutions. However, since component values are always positive values, we should select a valid solution to satisfy this condition.

Figure 6 shows the D-CRLH TL topology of the series-shunt type. The D-CRLH TL basically has a band-stop characteristic [22], and thus the dual-band impedance transformer using D-CRLH TL topology has narrow bandwidth, although the impedance transforming condition is satisfied. The D-CRLH TL consists of parallel resonance at series connection and series resonance at shunt connection. Hence, the equation of the component values of the D-CRLH TL can be applicable for other topologies such as series resonance and parallel resonance topology. The impedance of  $Z$  and the admittance of  $Y$  are obtained as

$$Z = jX_p = j \frac{1}{1/(\omega_s L_R) - \omega_s C_L}, \quad Y = jX_q = j \frac{1}{1/(\omega_s C_R) - \omega_s L_L} \quad (22)$$



**Figure 6.** D-CRLH TL topology for dual-band impedance transformer.



**Figure 7.** Series resonance topology for dual-band impedance transformer.

According to the same design process in the CRLH TL topology, the component values of the D-CRLH TL can be obtained as

$$C_R = 1 / \left( \omega_s \left( \frac{1}{X_{q1}} + \omega_s L_L \right) \right) \quad (23a)$$

$$C_L = \frac{K}{\omega_s(1 - K^2)} \left( \frac{1}{X_{p2}} - \frac{1}{KX_{p1}} \right) \quad (23b)$$

$$L_R = 1 / \left( \omega_s \left( \frac{1}{X_{p1}} + \omega_s C_L \right) \right) \quad (23c)$$

$$L_L = \frac{K}{\omega_s(1 - K^2)} \left( \frac{1}{X_{q2}} - \frac{1}{KX_{q1}} \right) \quad (23d)$$

Figure 7 shows the series resonance topology of the series-shunt type. It consists of series resonance at series connection and series resonance at shunt connection, and then it has only series resonance. Hence,  $C_L$  and  $L_R$ , which is series resonance at series connection, can be calculated by (21b) and (21c) and  $C_R$  and  $L_L$ , which is series resonance at shunt connection, can be calculated by (23a) and (23d).

Figure 8 shows the parallel resonance topology of the series-shunt type. It consists of parallel resonance at series connection and parallel resonance at shunt connection, and then it has only parallel resonance. Hence,  $C_L$  and  $L_R$ , which is parallel resonance at series connection, can be calculated by (23b) and (23c) and  $C_R$  and  $L_L$ , which is parallel resonance at shunt connection, can be calculated by (21a) and (21d).

The four topologies are introduced as above and the component values of these four topologies are obtained for the dual-band operation with frequency-dependent complex impedance loads. Hence, according to the proposed technique, the lumped dual-band impedance

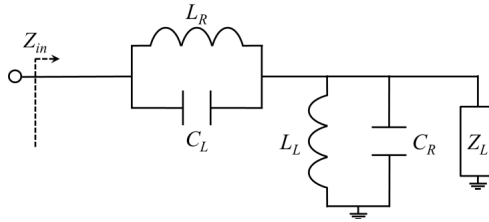


**Figure 8.** Parallel resonance topology for dual-band impedance transformer.

transformer can be realized for various complex loads with two types and combinations using four topologies.

#### 4. NUMERICAL EXAMPLES

Section 2 presents the input impedance for complex impedance transforming using the  $ABCD$  matrix and Section 3 presents the dual-band impedance transforming technique with lumped elements using the proposed equation of input impedance in Section 2. Hence, in order to verify the proposed technique, numerical examples are given. The numerical examples consist of the series-shunt and shunt-series type, the T- and the  $\pi$ -type combination using the CRLH TL topology. Furthermore, an example is given for complex loads of a transistor at the WLAN bands of 2.4 and 5 GHz. All numerical examples are matched to an input impedance  $Z_{in} = 50 \Omega$ .

##### 4.1. Series-shunt and Shunt-series Type with CRLH TL Topology

The closed-form design equations of the series-shunt and the shunt-series type were presented, and then the CRLH TL topology in Figure 5 is selected to verify the proposed dual-band transformers. These design parameters of the series-shunt and the shunt-series type are shown in Tables 1 and 2 with frequency-dependent complex loads, respectively. A first frequency  $f_1$  is fixed to 2 GHz and a second frequency  $f_2$  is varying from 3 to 5 GHz. Figure 9 shows the simulated reflection coefficients of various dual-band transformers in Tables 1 and 2. The complex loads are well matched to the input impedance at both designated frequencies in various cases of the series-shunt and the shunt-series type.

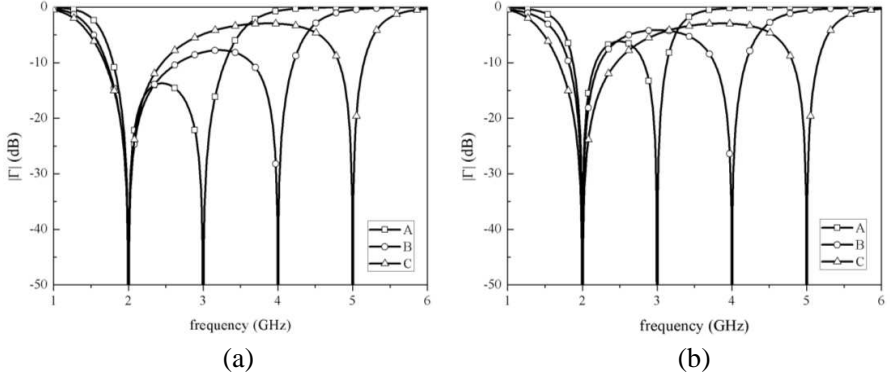


**Figure 9.** Reflection coefficients for dual-band transformer with CRLH TL topology: (a) series-shunt type, and (b) shunt-series type.

**Table 1.** Design parameters for dual-band transformer using series-shunt type with CRLH TL topology.

	$f_1/f_2$ (GHz)	$R_{L1}$ ( $\Omega$ )	$X_{L1}$ ( $\Omega$ )	$R_{L2}$ ( $\Omega$ )	$X_{L2}$ ( $\Omega$ )	$C_R$ (pF)	$C_L$ (pF)	$L_R$ (nH)	$L_L$ (nH)
A	2/3	71.696	17.784	52.959	44.335	2.2336	0.6701	6.5746	2.3198
B	2/4	71.696	17.784	38.773	76.941	1.1813	0.7634	5.42	3.7749
C	2/5	71.696	17.784	28.84	111.77	0.6478	0.7146	5.9869	5.5356

**Table 2.** Design parameters for dual-band transformer using shunt-series type with CRLH TL topology.

	$f_1/f_2$ (GHz)	$R_{L1}$ ( $\Omega$ )	$X_{L1}$ ( $\Omega$ )	$R_{L2}$ ( $\Omega$ )	$X_{L2}$ ( $\Omega$ )	$C_R$ (pF)	$C_L$ (pF)	$L_R$ (nH)	$L_L$ (nH)
A	2/3	24.435	-35.59	13.08	-27.7	4.511	1.9632	4.069	1.0315
B	2/4	24.435	-35.59	7.924	-21.38	2.9876	6.4698	1.8221	1.372
C	2/5	24.435	-35.59	5.259	-16.68	2.5206	30.22	1.0529	1.5264

#### 4.2. T- and $\pi$ -type Combination with CRLH TL Topology

The concept of combination is presented in Section 3. Figures 3 and 4 show the T- and  $\pi$ -type combination, respectively. The complex load is matched to  $Z_{in2}$  at midpoint, and then  $Z_{in2}$  is matched to the required input impedance  $Z_{in} = 50 \Omega$ . The design parameters of the T- and  $\pi$ -type combination for dual-band transformer with CRLH TL topology in Figure 5 are shown in Tables 3 and 4, respectively, where subscripts

**Table 3.** Design parameters for dual-band transformer using T-type combination with CRLH TL topology.

	$f_1/f_2$ (GHz)	$R_{L1}$ ( $\Omega$ )	$X_{L1}$ ( $\Omega$ )	$R_{L2}$ ( $\Omega$ )	$X_{L2}$ ( $\Omega$ )	$R_{in2-1}$ ( $\Omega$ )	$X_{in2-1}$ ( $\Omega$ )	$R_{in2-2}$ ( $\Omega$ )	$X_{in2-2}$ ( $\Omega$ )
A	2/3	63.756	-46.81	43.877	-47.73	150	0	55	0
B	2/4	63.756	-46.81	30.544	-43.54	150	0	55	0
C	2/5	63.756	-46.81	21.963	-38.25	150	0	55	0
	$f_1/f_2$ (GHz)	$C_{R-ses}$ (pF)	$C_{L-ses}$ (pF)	$L_{R-ses}$ (nH)	$L_{L-ses}$ (nH)	$C_{R-shs}$ (pF)	$C_{L-shs}$ (pF)	$L_{R-shs}$ (nH)	$L_{L-shs}$ (nH)
A	2/3	1.1493	0.5441	6.0115	3.3338	1.3678	0.5983	8.4088	3.1905
B	2/4	0.5551	0.7592	2.7145	4.8511	1.0688	0.9507	4.4853	3.7564
C	2/5	0.3608	0.8677	1.671	5.6996	0.9625	1.2514	2.8849	4.0091

**Table 4.** Design parameters for dual-band transformer using  $\pi$ -type combination with CRLH TL topology.

	$f_1/f_2$ (GHz)	$R_{L1}$ ( $\Omega$ )	$X_{L1}$ ( $\Omega$ )	$R_{L2}$ ( $\Omega$ )	$X_{L2}$ ( $\Omega$ )	$R_{in2-1}$ ( $\Omega$ )	$X_{in2-1}$ ( $\Omega$ )	$R_{in2-2}$ ( $\Omega$ )	$X_{in2-2}$ ( $\Omega$ )
A	2/3	77.545	-34.61	43.927	11.448	40	0	30	0
B	2/4	77.545	-34.61	27.335	56.963	40	0	10	0
C	2/5	77.545	-34.61	18.4	99.275	40	0	5	0
	$f_1/f_2$ (GHz)	$C_{R-ses}$ (pF)	$C_{L-ses}$ (pF)	$L_{R-ses}$ (nH)	$L_{L-ses}$ (nH)	$C_{R-shs}$ (pF)	$C_{L-shs}$ (pF)	$L_{R-shs}$ (nH)	$L_{L-shs}$ (nH)
A	2/3	3.1524	0.7241	5.082	1.4012	2.196	1.2169	3.6123	2.1167
B	2/4	2.5525	0.9255	3.178	1.6157	2.3873	1.9894	1.5915	1.9894
C	2/5	1.3461	0.9977	2.6833	2.3341	2.4252	2.571	0.8716	1.966

of *ses* and *shs* indicate series-shunt and shunt-series type, respectively.  $Z_{in2-1}$  and  $Z_{in2-2}$  are input impedances of midpoint at  $f_1$  and  $f_2$ , respectively. Figure 10 shows the simulated reflection coefficients of various cases in Tables 3 and 4 with the excellent results.

Here, in terms of the T-type, the number of parallel lumped elements at midpoint is 4, which consists of two capacitances and two inductances, because it uses a two-stage dual-band transformer. However, as above in Section 3, it can be reduced to 2 by their synthesis, when the CRLH TL topology is used, because it consists of only parallel resonance at shunt connection. Likewise, in the  $\pi$ -type it can be also reduced. Hence, although the combination types are used, they can use limited number of lumped elements in the CRLH TL topology.

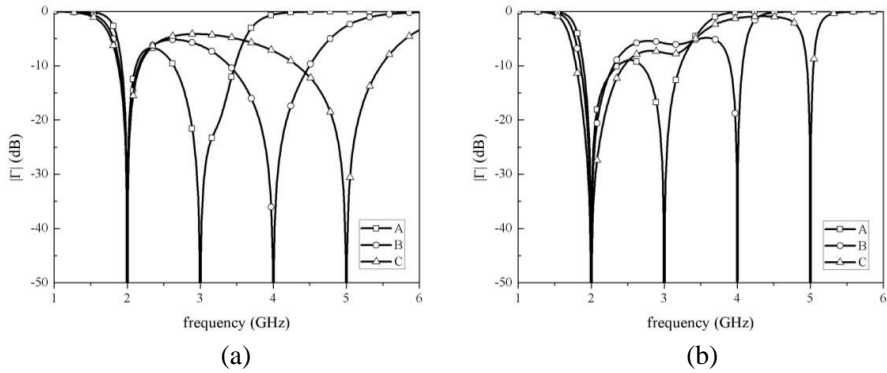


**Figure 10.** Reflection coefficients for dual-band transformer with CRLH TL topology: (a) T-type combination, and (b)  $\pi$ -type combination.

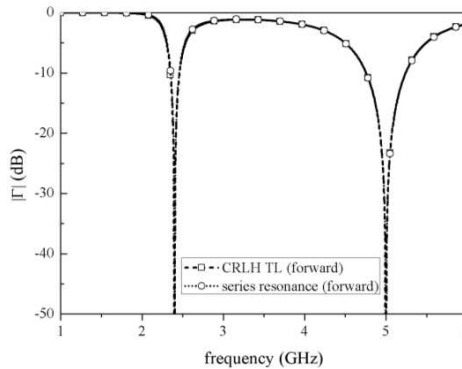


**Figure 11.** Reflection coefficients for dual-band transformer with loads of transistor.

### 4.3. Example for Transistor

A transistor of NE3210S01 from NEC is examined at WLAN bands of 2.4 and 5 GHz. In this case, the series-shunt type is suitable for complex impedance transforming and it has available solutions when the CRLH TL and the series resonance topology are used.

These design parameters for dual-band transformer are shown in Table 5, and Figure 11 shows the simulated reflection coefficients of various cases in Table 5 where A and B are the CRLH TL and the series resonance topology of the series-shunt type, respectively. According to Figure 11, the complex loads of the transistor are well matched to the input impedance at both designated frequencies in the two topologies.

**Table 5.** Design parameters for dual-band transformer.

	$f_1/f_2$ (GHz)	$R_{L1}$ ( $\Omega$ )	$X_{L1}$ ( $\Omega$ )	$R_{L2}$ ( $\Omega$ )	$X_{L2}$ ( $\Omega$ )	$C_R$ (pF)	$C_L$ (pF)	$L_R$ (nH)	$L_L$ (nH)
A	2.4/5	24.980	-172.6	25.022	-72.32	0.0172	8.7029	0.1778	6.6973
B	2.4/5	24.980	-172.6	25.022	-72.32	4.9902	8.7029	0.1778	7.7585

## 5. CONCLUSION

In this study, the dual-band impedance transforming technique for arbitrary frequency-dependent complex loads has been developed. This technique uses the proposed equation of input impedance, which can easily obtain the input impedance of any two-port network using the  $ABCD$  matrix. For the complex impedance transformer, the series-shunt and the shunt-series types and the combinations are presented. They are comprised of four topologies, and then the analysis is presented for dual-band operation. The numerical examples demonstrate the exactness, feasibility and versatility of the proposed technique with limited number of lumped elements. The proposed technique is applicable in practical matching problems, such as microwave amplifiers and other devices.

## REFERENCES

1. Chow, Y. L. and K. L. Wan, "A transformer of one-third wavelength in two sections-for a frequency and its first harmonic," *IEEE Microwave Wireless Components Letters*, Vol. 12, No. 1, 22–23, Jan. 2002.
2. Monzon, C., "A small dual-frequency transformer in two sections," *IEEE Transaction on Microwave Theory Techniques*, Vol. 51, No. 4, 1157–1161, Apr. 2003.
3. Wu, Y., Y. Liu, and S. Li, "A Compact pi-structure dual band transformer," *Progress In Electromagnetics Research*, Vol. 88, 121–134, 2008.
4. Sophocles, J. and A. Orfanidis, "Two-section dual-band Chebyshev impedance transformer," *IEEE Microwave Wireless Components Letters*, Vol. 13, No. 9, 382–384, Sep. 2003.
5. Castaldi, G., V. Fiumara, and I. Gallina, "An exact synthesis method for dual-band Chebyshev impedance transformers," *Progress In Electromagnetics Research*, Vol. 86, 305–319, 2008.
6. Kuo, J.-T., C.-Y. Fan, and S.-C. Tang, "Dual-wideband bandpass

- filters with extended stopband based on coupled-line and coupled three-line resonators,” *Progress In Electromagnetics Research*, Vol. 124, 1–15, 2012.
7. Wu, L., Z. Sun, H. Yilmaz, and M. Berroth, “A dual-frequency Wilkinson power divider,” *IEEE Transaction on Microwave Theory Techniques*, Vol. 54, No. 1, 278–284, 2006.
  8. Li, B., X. Wu, N. Yang, and W. Wu, “Dual-band equal/unequal Wilkinson power dividers based on coupled-line section with short-circuited stub,” *Progress In Electromagnetics Research*, Vol. 111, 163–178, 2011.
  9. Li, J. C., Y. L. Wu, Y. A. Liu, J. Y. Shen, S. L. Li, and C. P. Yu, “A generalized coupled-line dual-band Wilkinson power divider with extended ports,” *Progress In Electromagnetics Research*, Vol. 129, 197–214, 2012.
  10. Fagotti, R., A. Cidronali, and G. Manes, “Concurrent hex-band GaN power amplifier for wireless communication systems,” *IEEE Microwave and Wireless Components Letters*, Vol. 21, No. 2, 89–91, 2011.
  11. Chen, W., S. A. Bassam, X. Li, Y. Liu, K. Rawat, M. Helaoui, F. M. Ghannouchi, and Z. Feng, “Design and linearization of concurrent dual-band Doherty power amplifier with frequency-dependent power ranges,” *IEEE Transaction on Microwave Theory and Techniques*, Vol. 59, No. 10, 2537–2546, Oct. 2011.
  12. Chen, X. Q., X. W. Shi, Y. C. Guo, and C. M. Xiao, “A novel dual band transmitter using microstrip defected ground structure,” *Progress In Electromagnetics Research*, Vol. 83, 1–11, 2008.
  13. Wu, Y., Y. Liu, and S. Li, “A dual-frequency transformer for complex impedances with two unequal sections,” *IEEE Microwave Wireless Components Letters*, Vol. 19, No. 2, 77–79, 2009.
  14. Liu, X., Y. Liu, S. Li, F. Wu, and Y. Wu, “A three-section dual-band transformer for frequency-dependent complex load impedance,” *IEEE Microwave Wireless Components Letters*, Vol. 19, No. 10, 611–613, Oct. 2009.
  15. Chuang, M. L., “Dual-band impedance transformer using two-section shunt stubs,” *IEEE Transaction on Microwave Theory Techniques*, Vol. 58, No. 5, 1257–1263, May 2010.
  16. Nikravan, M. A. and Z. Atlasbaf, “T-section dual-band impedance transformer for frequency-dependent complex loads,” *Electronics Letters*, Vol. 47, No. 9, 551–553, Apr. 2011.
  17. Li, S., B. H. Tang, Y. A. Liu, S. L. Li, C. P. Yu, and Y. L. Wu, “Miniaturized dual-band matching technique based on coupled-

- line transformer for dual-band power amplifiers design,” *Progress In Electromagnetics Research*, Vol. 131, 195–210, 2012.
18. Liu, Y., Y.-J. Zhao, and Y. Zhou, “Lumped dual-frequency impedance transformers for frequency-dependent complex loads,” *Progress In Electromagnetics Research*, Vol. 126, 121–138, 2012.
  19. Pozar, D. M. *Microwave Engineering*, 3rd Edition, Wiley, New York, 2005.
  20. Medley, M. W., *Microwave and RF Circuits: Analysis, Synthesis, and Design*, Artech House, 1993.
  21. Caloz, C. and T. Itoh, *Electromagnetic Metamaterials: Transmission Line Theory and Microwave Applications*, Wiley, New York, 2006.
  22. Caloz, C., “Dual composite right/left-handed (D-CRLH) transmission line metamaterial,” *IEEE Microwave and Wireless Components Letters*, Vol. 16, No. 11, 585–587, Nov. 2006.